Supporting Information for:

Identification of the Inhibitory Mechanism of FDA Approved Selective Serotonin Reuptake Inhibitors: Insight from a Molecular Dynamics Simulation Study

Weiwei Xue[1], Panpan Wang[1], Bo Li[1], Yinghong Li[1], Xiaofei Xu[1], Fengyuan Yang[1], Xiaojun Yao[2], Yuzong Chen[3], Feng Xu[4]*, Feng Zhu[1]*

[1] Innovative Drug Research and Bioinformatics Group, Innovative Drug Research Centre and College of Chemistry and Chemical Engineering, Chongqing University, Chongqing 401331, China

[2] State Key Laboratory of Applied Organic Chemistry and Department of Chemistry, Lanzhou University, Lanzhou 730000, China

[3] Bioinformatics and Drug Design Group, Department of Pharmacy, National University of Singapore 117543, Singapore

[4] College of Pharmacy and Tianjin Key Laboratory of Molecular Drug Research, Nankai University, Tianjin 300071, China

* Corresponding authors: Feng Zhu (zhufeng@cqu.edu.cn) and Feng Xu (xufeng@nankai.edu.cn)

Supporting Information for METHODS

Molecular Docking

To obtain the initial binding mode of 4 studied SSRIs (fluoxetine, sertraline, paroxetine and escitalopram) to hSERT, molecular docking was carried out using Glide software[1], with default settings of standard precision mode. The 3D structures of these 4 SSRIs were retrieved from the PubChem database. Then, structures of 4 SSRIs were preprocessed by the LigPrep[2] using OPLS-2005 force field[3] and resulted in a low energy conformation. The ionized state was assigned by Epik[4] at a pH value of 7.0 ± 2.0.

To prepare hSERT structure for docking, the Protein Preparation Wizard module in Maestro[5] was used to add hydrogen atoms, assign partial charges using OPLS-2005 force field, assign protonation states and minimize the structure. The minimization was terminated when the root mean square deviation reached the maximum value of 0.30 Å. Site-directed mutagenesis study showed that Tyr95, Asp98, Ile172, Asn177, Phe341 and Ser438 of hSERT are critical for SSRIs' binding[6]. Therefore, a docking grid box was defined using the Receptor Grid Generation tool in Glide by centering these six residues in the modeled structure of hSERT. In molecular docking, 5000 poses were generated during the initial phase of the docking calculation, out of which best 400 poses were chosen for energy minimization by 100 steps of conjugate gradient minimizations.

Cross-Docking

To test the effectiveness of molecular docking, the X-ray structures of LeuBAT in complex with fluoxetine, sertraline and paroxetine (PDB codes 4MM8, 4MM5 and 4MM4) were used for cross-docking by Glide software[1]. The ligands and proteins were firstly prepared in the same way as described above. Then, the docking grid boxes were defined by centering on fluoxetine, sertraline or paroxetine in LeuBAT using the Receptor Grid Generation tool in Glide[1]. Finally, the prepared fluoxetine, sertraline and paroxetine were cross-docked into the corresponding fluoxetine, sertraline and paroxetine bound LeuBAT structures using the same parameter settings for 4 SSRIs' molecular docking.

Protein-Ligand/Membrane System Setup

Coordinates of four obtained SSRIs-hSERT structures were pre-oriented in OPM[7] with respect to the Membrane Normal which is defined by the Z-axis. Then SSRIs-hSERT complexes were embedded into the explicit POPC lipid bilayer using the Membrane Builder

module of CHARMM-GUI[8-11].

The TIP3P water[12] of 20Å thickness was placed above and below the membrane and the salt concentration was kept at 0.15M by adding Na^+ and Cl^-. The overall system contained a total of ~96000 atoms per periodic cell. The box size was set as $83\text{Å} \times 83\text{Å} \times 127\text{Å}$.

MD simulation

MD simulation was performed within the AMBER14[13] using GPU-accelerated PMEMD on 16 cores of an array of two 2.6GHz Intel Xeon E5-2650v2 processors and 4 pieces of NVDIA Tesla NVIDIA Tesla K20C graphics card.

AMBER force field *ff14SB*[14] and *Lipid14*[15] were used for protein and lipids, respectively. The ions parameters for TIP3P water are collected from Joung & Cheatham[16]. The force field parameters for fluoxetine, sertraline, escitalopram, paroxetine and cholesterol were described by the General AMBER Force Field[17] and the charges were assigned using Restrained Electrostatic Potential partial charges[18] with Antechamber[19]. Geometry optimization and the electrostatic potential calculations were performed with Gaussian09 at the HF/6-31G* level[20].

Prior to MD simulation, the prepared systems were subjected to initial energy minimization by two steps. The first step is to apply harmonic restraints with a force constant of 10.0 kcal/(mol·Å^2) to the lipid and solute atoms, and the second step is to allow all atoms to move freely. In each step, energy minimization was performed by the steepest descent method for the first 5000 steps and the conjugated gradient method for the subsequent 5000 steps. After the initial minimization, the system was heated through two sequential runs to 310K while keeping the lipid and solute atoms fixed over 100ps in the NVT ensemble. Firstly, the system is heated to 100K and then gradually to 310 K. Subsequently, 10 times unconstrained equilibration (5ns) at 310K were performed to equilibrate the system's periodic boundary condition. Finally, 150ns MD simulation was conducted in NPT ensemble under a temperature of 310K and a pressure of 1 atm. Temperature is controlled here using Langevin dynamics while pressure is controlled using the anisotropic Monte Carlo barostat included in AMBER14.

In the MD simulations, periodic boundary conditions were employed and direct space interaction was calculated by considering the long range electrostatic interaction (cutoff = 10.0Å) using particle-mesh Ewald method[21]. Here, the dimension of periodic box was measured using VMD 1.9.1[22]. All bonds involving hydrogen atoms were constrained with the

SHAKE algorithm[23] allowing an integration time step of 2 fs.

All MD trajectories analysis, such as the root mean square deviation between structure pairs and the extraction of representative structures from trajectories, were performed using *cpptraj*[24] as implemented in AMBER14. Visualization of structures was performed with PyMOL[25].

Binding Free Energy Calculation

The relative binding free energies of SSRIs on the wild type and mutant hSERT were calculated using the single-trajectory based MM/GBSA method[26, 27]. The *mm_pbsa.pl* under AMBER14 was used to carry out the MM/GBSA calculation. A total of 500 snapshots were taken from the last 50 ns equilibrium trajectory of each complex. For each snapshot, all of the ions (except for the functional ions in the binding site), lipid, and water molecules were removed. The MM/GBSA binding free energy ($\Delta G_{MM/GBSA}$) calculated by excluding entropic contribution is given by

$$\Delta G_{MM/GBSA} = \Delta E_{vdW} + \Delta E_{ele} + \Delta G_{pol} + \Delta G_{nonpol} \quad (1)$$

In Eq. (1), ΔE_{vdW} and ΔE_{ele} represent the van der Waals and electrostatic components in gas phase, and ΔG_{pol} and ΔG_{nonpol} stand for polar and non-polar solvent interaction energies. ΔE_{vdW} and ΔE_{ele} were calculated using the AMBER force field ff14SB, and the electrostatic free energy of solvation (ΔG_{pol}) were calculated by the modified GB model (igb = 2) developed by Onufriev et al.[28]. The solute and solvent dielectric constants were set to 2 and 80, respectively. The nonpolar solvation free energy (ΔG_{nonpol}) was calculated from the solvent accessible area (SASA) using the linear combination of pairwise overlaps (LCPO) method ($\Delta G_{nonpol} = 0.0072 \times \Delta SASA$). SASA here was determined with probe radii of 1.4 Å[29].

Per-residue Free Energy Decomposition Analysis

To quantitatively evaluate the contribution to SSRIs' binding, the total binding free energy was decomposed on a per-residue basis, which including contributions from the van der Waals term ($\Delta E^{per-residue}_{vdW}$), electrostatic term ($\Delta E^{per-residue}_{ele}$), polar term ($\Delta G^{per-residue}_{pol}$) and nonpolar term ($\Delta G^{per-residue}_{nonpol}$) for the ligand and each residue, as shown in Eq. (2):

$$\Delta G^{per-residue}_{MM/GBSA} = \Delta E^{per-residue}_{vdW} + \Delta E^{per-residue}_{ele} + \Delta G^{per-residue}_{pol} + \Delta G^{per-residue}_{nonpol} \quad (2)$$

where $\Delta E_{vdW}^{per-residue}$, $\Delta E_{ele}^{per-residue}$ and $\Delta G_{pol}^{per-residue}$ were calculate using the same approach in "Binding Free Energy Calculation" section, while the non-polar term was estimated as $\Delta G_{nonpol}^{per-residue} = 0.0072 \times \Delta SASA$ based on the recursive approximation of a sphere around an atom, starting from an icosahedron (ICOSA)[13].

Table S1. Comparison between the calculated and experimental binding free energies for 4 SSRIs to the wild type and mutant hSERT (All energies are in kcal/mol, all K_i values are in nM, and mutation induced $\geq$ 10-fold shift in the inhibitory potency (K_i) for SSRIs binding)

Systems		ΔE_{ele}[a]	ΔE_{vdW}[a]	ΔG_{pol}[a]	ΔG_{nonpol}[a]	$\Delta G_{MM/GBSA}$[a]	ΔG_{exp}[b]	K_i[c]
	Wild Type	**-19.65 ± 0.19**	**-39.79 ± 0.11**	**23.53 ± 0.16**	**-5.61 ± 0.0054**	**-41.52 ± 0.10**	**-9.00**	**255 ± 61**
Fluoxetine	Tyr/Ala95	-16.83 ± 0.14	-38.22 ± 0.10	23.95 ± 0.10	-5.35 ± 0.0071	-36.44 ± 0.10	-7.58	2830 ± 177
	Ile/Met172	-21.93 ± 0.18	-39.14 ± 0.11	27.95 ± 0.14	-5.63 ± 0.0076	-38.74 ± 0.097	-7.32	4304 ± 929
Sertraline	**Wild Type**	**-16.74 ± 0.22**	**-41.99 ± 0.12**	**19.43 ± 0.15**	**-5.02 ± 0.0067**	**-44.32 ± 0.12**	**-9.03**	**242 ± 33**
	Ser/Thr438	-27.35 ± 0.17	-37.55 ± 0.12	26.51 ± 0.14	-5.04 ± 0.0062	-43.43 ± 0.10	-7.08	6551 ± 1435
Escitalopram	**Wild Type**	**-31.98 ± 0.20**	**-47.66 ± 0.11**	**36.67 ± 0.17**	**-6.24 ± 0.0058**	**-49.21 ± 0.12**	**-10.23**	**32 ± 1**
	Tyr/Ala95	-18.04 ± 0.17	-51.17 ± 0.11	27.96 ± 0.15	-6.30 ± 0.0058	-47.55 ± 0.10	-8.72	408 ± 54
	Asp/Glu98	-22.01 ± 0.18	-48.53 ± 0.11	29.20 ± 0.13	-6.24 ± 0.0058	-47.57 ± 0.11	-8.29	856 ± 117
	Ile/Met172	-22.30 ± 0.18	-46.61 ± 0.10	28.41 ± 0.14	-6.10 ± 0.0062	-46.59 ± 0.11	-6.63	13946 ± 3167
	Phe/Tyr341	-31.87 ± 0.16	-42.62 ± 0.12	34.67 ± 0.14	-6.20 ± 0.0067	-46.02 ± 0.11	-7.88	1691 ± 208
	Ser/Thr438	-17.40 ± 0.22	-49.11 ± 0.10	25.08 ± 0.19	-6.39 ± 0.0054	-47.82 ± 0.11	-6.98	7693 ± 874
Paroxetine	**Wild Type**	**-45.05 ± 0.16**	**-45.93 ± 0.13**	**46.10 ± 0.14**	**-6.27 ± 0.0058**	**-51.14 ± 0.12**	**-10.40**	**24 ± 6**
	Tyr/Ala95	-33.35 ± 0.14	-46.58 ± 0.13	37.09 ± 0.11	-6.04 ± 0.0067	-48.88 ± 0.12	-7.85	1759 ± 306
	Asp/Glu98	-28.49 ± 0.16	-49.78 ± 0.12	33.83 ± 0.13	-6.29 ± 0.0044	-50.72 ± 0.12	-9.16	195 ± 37
	Phe/Tyr341	-42.43 ± 0.14	-47.68 ± 0.12	44.88 ± 0.12	-6.23 ± 0.0058	-51.45 ± 0.11	-8.37	741 ± 73
	Ser/Thr438	-24.47 ± 0.14	-52.23 ± 0.12	30.65 ± 0.12	-6.28 ± 0.0049	-52.33 ± 0.12	-7.56	2885 ± 559

[a] Calculated binding free energy in this work.

[b] Estimated binding free energy based on K_i values using $\Delta G_{exp} = -RTln(K_i)$.

[c] Experimental value from Sørensen's work[30].

Table S2. The calculated contributions of hot spot residues for fluoxetine's binding[a]

Drug	hSERT Residues	Systems			
		Wild Type	Tyr/Ala95	Ile/Met172	Asn/Ser177
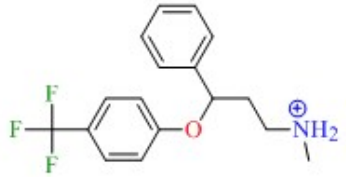 Fluoxetine	**Tyr/Ala95**	**-3.68**	**0.05**	**-3.38**	**-3.77**
	Ala96	-0.64	-0.69	-0.73	-0.63
	Asp98	-2.75	-2.64	-2.61	-2.88
	Ile/Met172	**-2.85**	**-3.10**	**-2.91**	**-2.85**
	Ala173	-0.57	-0.53	-0.53	-0.53
	Tyr176	-1.95	-2.05	-1.08	-1.86
	Phe341	-0.94	-0.70	-1.26	-0.63
	Asp437	-0.36	-0.52	-0.39	-0.40
	Ser438	-1.44	-2.13	-1.08	-1.40
	Thr439	-1.69	-1.62	-1.41	-1.64
	Gly442	-0.89	-1.04	-0.95	-0.99
	Leu443	-0.69	-0.78	-0.65	-0.75

[a] All values are given in kcal/mol.

Table S3. The calculated contributions of hot spot residues for sertraline's binding[a]

Drug	hSERT Residues	Systems	
		Wild Type	Ser/Thr438
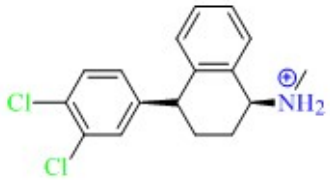 Sertraline	Tyr95	-1.87	-2.66
	Asp98	-2.13	-1.68
	Ala169	-0.77	-0.89
	Ile172	-2.2	-1.66
	Ala173	-0.73	-0.49
	Tyr176	-2.7	-1.36
	Phe341	-1.84	-1.66
	Asp437	-0.36	-0.35
	Ser/Thr438	**-1.3**	**-2.15**
	Thr439	-1.87	-1.47
	Gly442	-1.14	-0.76
	Leu443	-0.93	-0.98

[a] All values are given in kcal/mol.

Table S4. The calculated contributions of hot spot residues for escitalopram's binding[a]

Drug	hSERT Residues	Systems						
		Wild Type	Tyr/Ala95	Asp/Glu98	Ile/Met172	Asn/Ser177	Phe/Tyr341	Ser/Thr438
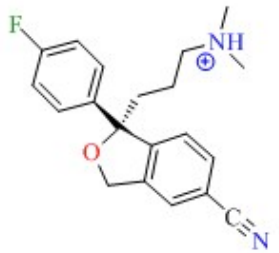 Escitalopram	**Tyr/Ala95**	**-2.36**	**-0.21**	**-3.36**	**-3.34**	**-3.61**	**-2.21**	**-3.23**
	Ala96	-0.43	-0.35	-0.57	-0.64	-0.54	-0.39	-0.57
	Asp/Glu98	**-1.83**	**-1.43**	**-0.93**	**-0.73**	**-1.81**	**-2.01**	**-0.99**
	Leu99	-1	-0.94	-0.11	-0.1	-0.13	-0.18	-0.07
	Gly100	-0.51	-0.25	-0.01	-0.05	-0.06	-0.16	0.02
	Trp103	-0.52	-0.13	-0.01	-0.01	-0.04	-0.15	0
	Ile/Met172	**-2.26**	**-2.17**	**-3.05**	**-2.6**	**-3.13**	**-2.3**	**-3.05**
	Ala173	-0.5	-0.34	-0.5	-0.61	-0.5	-0.58	-0.42
	Tyr175	-0.5	-0.37	-0.5	-0.39	-0.7	-0.68	-0.4
	Tyr176	-2.41	-2.25	-2.01	-2.01	-2.33	-1.99	-1.64
	Phe334	-0.31	-0.97	-0.43	-0.32	-0.19	-0.27	-0.33
	Phe335	-1.99	-2.19	-1.69	-1.69	-0.54	-1.94	-1.94
	Ser336	-0.7	-0.7	-0.49	-0.5	-0.54	-0.57	-0.41
	Gly338	-0.61	-0.7	-0.75	-0.59	-0.71	-0.56	-0.67
	Phe/Tyr341	**-1.86**	**-3.23**	**-1.11**	**-1.63**	**-1.06**	**-0.48**	**-1.62**
	Ser/Thr438	**-2.08**	**-1.43**	**-0.95**	**-0.95**	**-0.94**	**-1.03**	**-1.17**
	Thr439	-1.06	-1.18	-1.33	-1.22	-1.46	-0.98	-1.29
	Gly442	-0.2	-0.54	-0.73	-1.13	-1.11	-0.68	-1.21
	Val501	-0.13	-0.11	-0.66	-0.5	-0.4	-0.29	-0.79

[a] All values are given in kcal/mol.

Table S5. The calculated contributions of hot spot residues for paroxetine's binding[a]

Drug	hSERT Residues	Systems				
		Wild Type	Tyr/Ala95	Asp/Glu98	Phe/Tyr341	Ser/Thr438
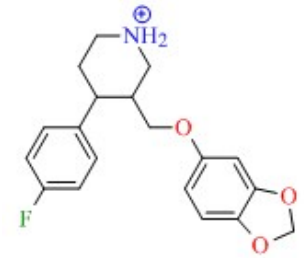 Paroxetine	**Tyr/Ala95**	**-3.31**	**-1.26**	**-3.84**	**-4.09**	**-3.97**
	Asp/Glu98	**-2.38**	**-3.79**	**-1.81**	**-1.86**	**-1.10**
	Ala169	-0.78	-0.62	-1.01	-0.98	-1.16
	Ile172	-2.74	-2.15	-2.92	-2.45	-2.82
	Ala173	-0.86	-0.51	-0.45	-0.63	-0.45
	Tyr176	-1.98	-1.57	-1.67	-1.34	-1.60
	Phe334	-0.25	-0.87	-0.55	-0.15	-0.77
	Phe335	-0.42	-0.53	-0.37	-0.47	-1.60
	Ser336	-0.71	-0.33	-1.29	-0.68	-1.84
	Gly338	-0.36	-0.91	-0.72	-0.50	-0.63
	Phe/Tyr341	**-1.74**	**-0.77**	**-0.62**	**-1.63**	**-2.03**
	Val343	-0.50	-0.47	-0.24	-0.75	-0.51
	Ser/Thr438	**-0.88**	**-1.21**	**-0.71**	**-0.87**	**-0.95**
	Thr439	-1.22	-0.89	-1.12	-1.36	-0.92
	Gly442	-1.18	-0.99	-1.16	-1.15	-1.12
	Leu443	-1.20	-0.94	-1.19	-1.43	-0.91
	Thr497	-0.60	-1.09	-1.02	-0.54	-0.40

[a] All values are given in kcal/mol.

Figure S1. Sequence alignment between hSERT (from Glu78 to Pro617) and dDAT (from Glu26 to Asp599) using ClustalW2 program[31]. The 12 transmembrane (TM1 to TM12) alpha helices are labeled above the sequence. Stars refer to the identical residues, the double filled periods refer to the conservative substitutions and the filled periods refer to the variable conservative substitutions.

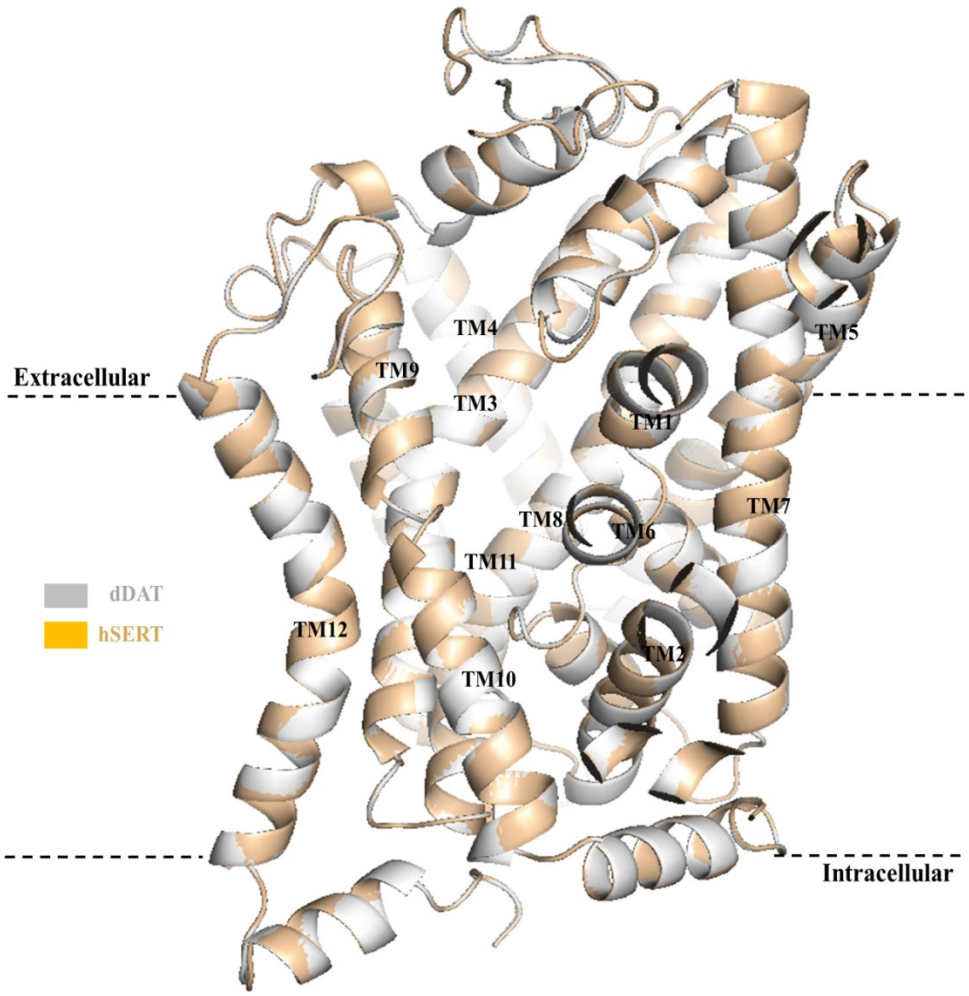

Figure S2. Structural superimposition between hSERT model and the crystal structure of dDAT (PDB code 4M48). hSERT and dDAT are shown in cartoon representation in light brown and gray, respectively.

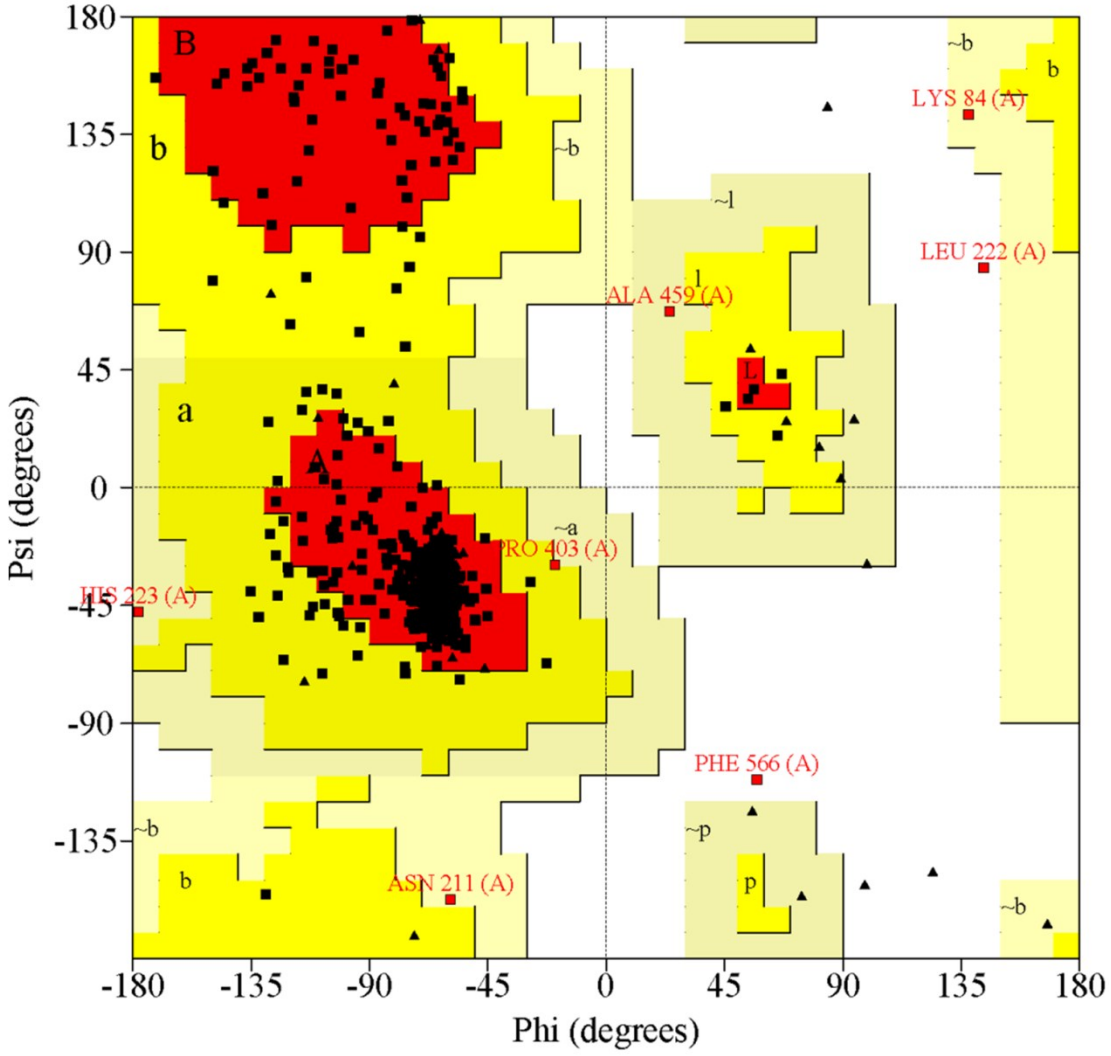

Plot statistics

Residues in most favoured regions [A,B,L]	417	87.6%
Residues in additional allowed regions [a,b,l,p]	53	11.1%
Residues in generously allowed regions [~a,~b,~l,~p]	4	0.8%
Residues in disallowed regions	2	0.4%
Number of non-glycine and non-proline residues	476	100.0%
Number of end-residues (excl. Gly and Pro)	0	
Number of glycine residues (shown as triangles)	42	
Number of proline residues	23	
Total number of residues	541	

Figure S3. Ramachandran plot of the hSERT model.

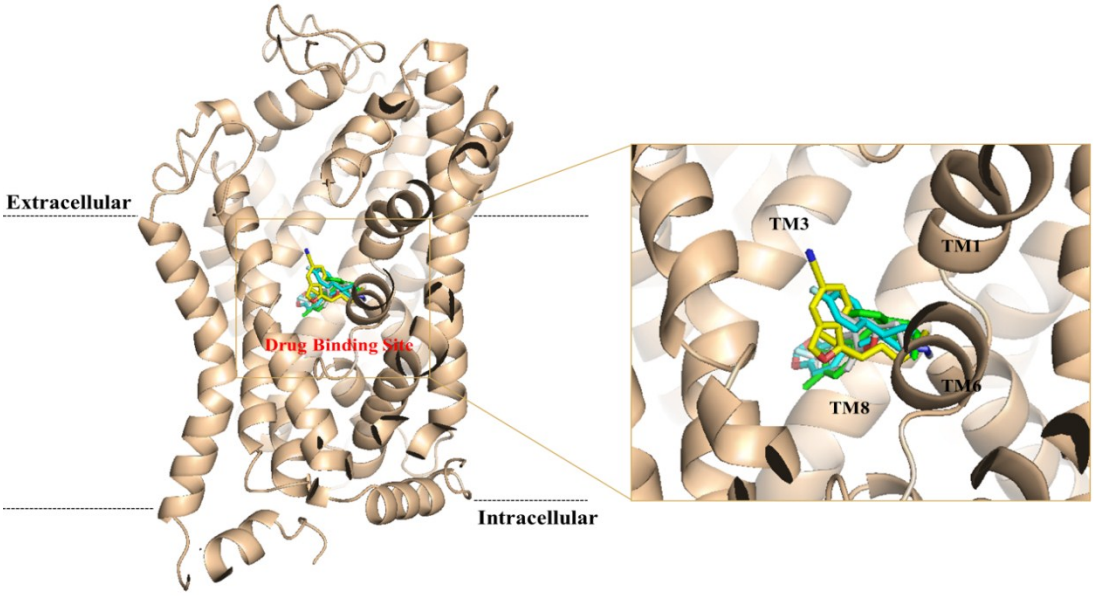

Figure S4. Docked poses of SSRIs fluoxetine, sertraline, paroxetine and escitalopram in the binding pocket of the modeled hSERT. hSERT is shown in ribbon representation in light brown. Fluoxetine, sertraline, escitalopram and paroxetine are shown as gray, green, yellow, and cyan sticks, respectively.

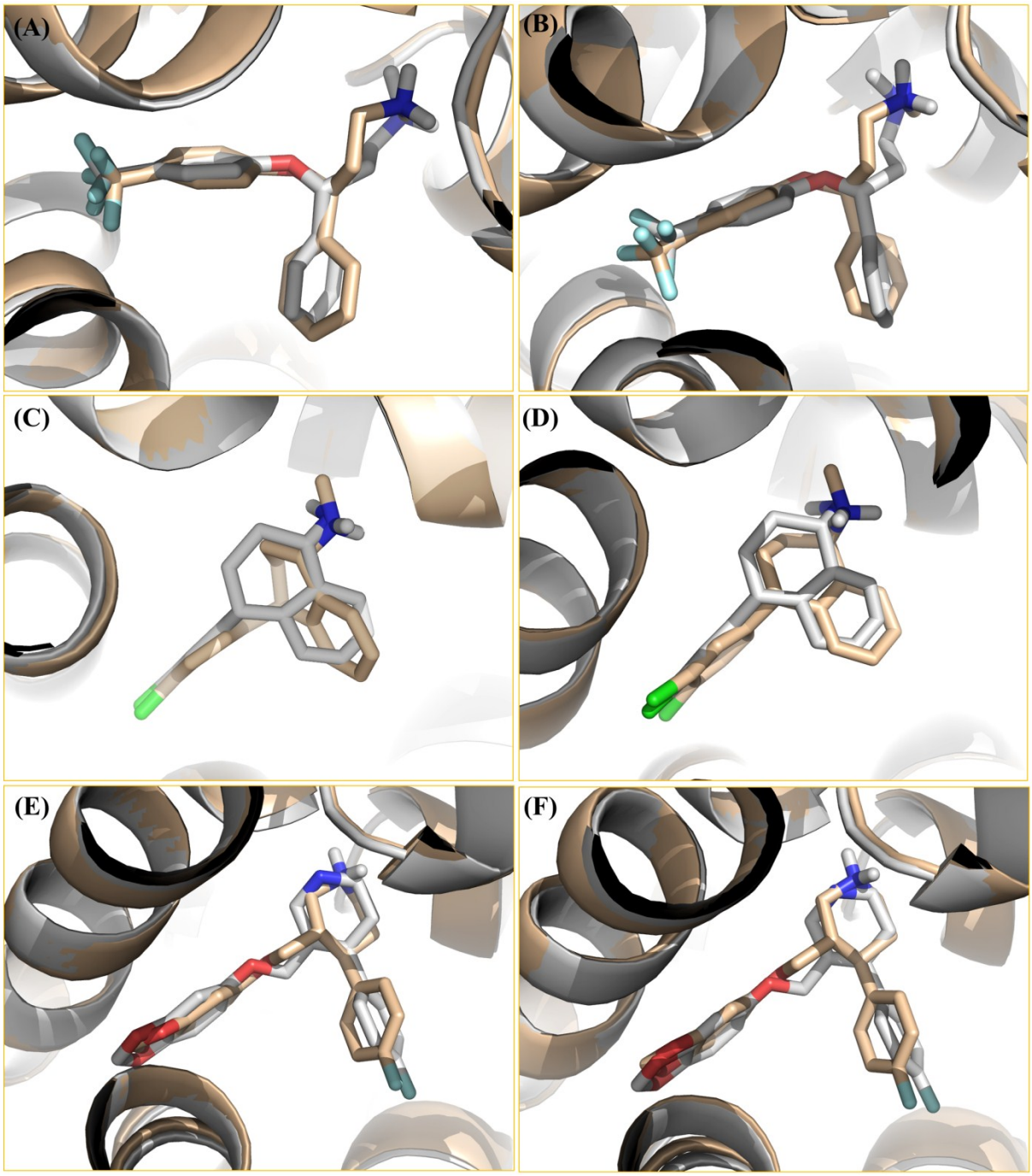

Figure S5. Structural superimposition between the cross-docking poses (light brown) of fluoxetine, sertraline and paroxetine with its corresponding co-crystal pose (gray) in LeuBAT.

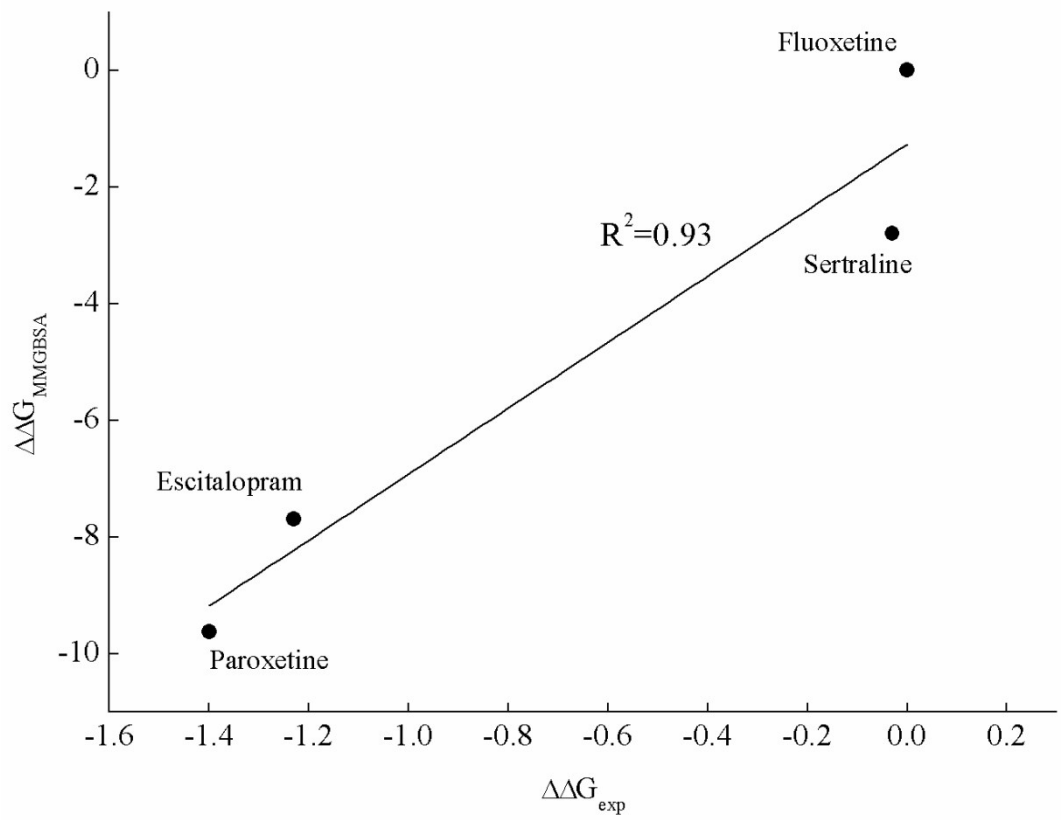

Figure S6. Correlation of differences of energies calculated in this study ($\Delta\Delta G_{MM/GBSA}$) and estimated based on experiments ($\Delta\Delta G_{exp}$).

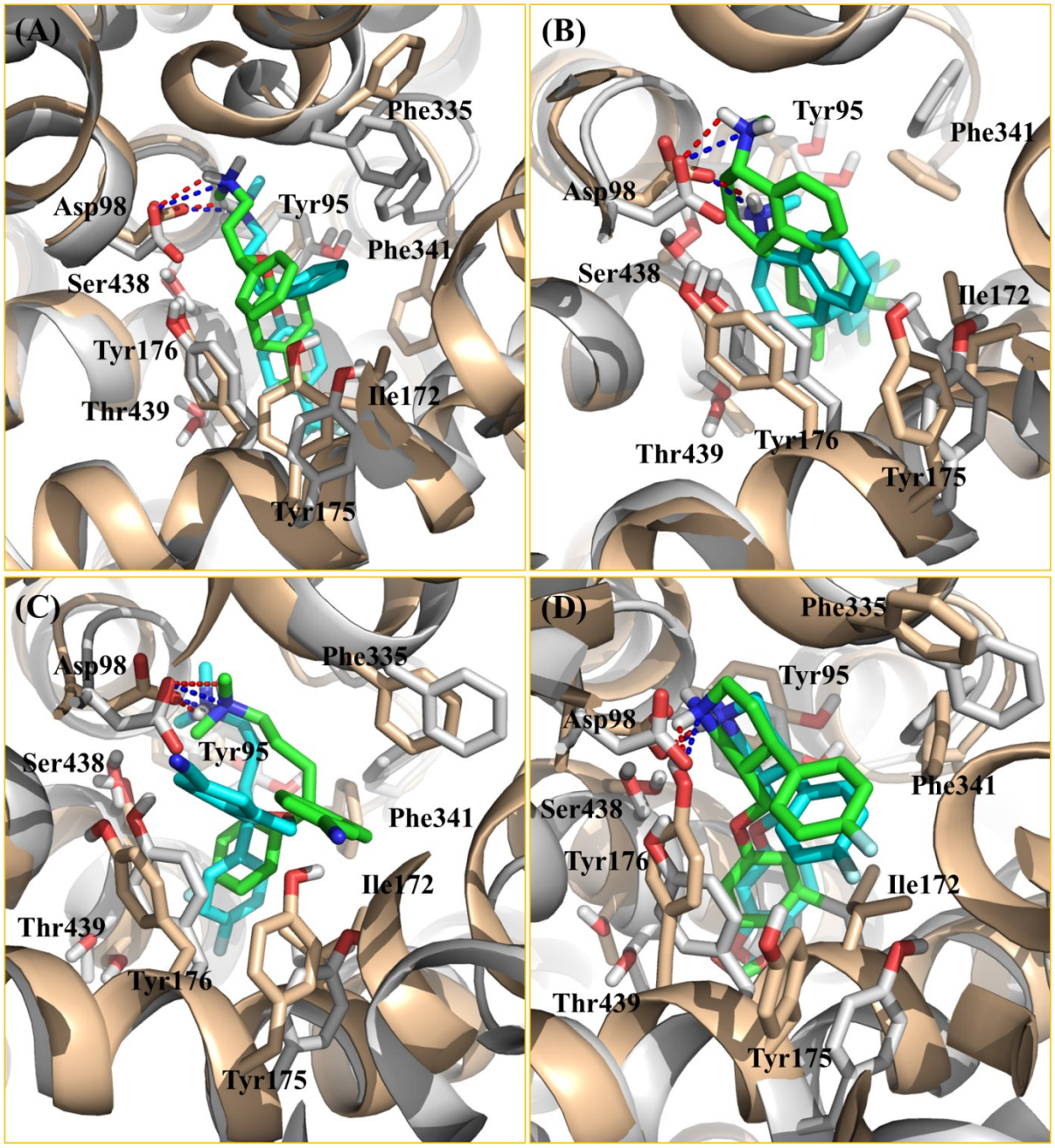

Figure S7. Structural alignment of the docking poses of SSRIs-hSERT and their corresponding representative snapshots from equilibrated MD trajectories. SSRIs in the docked and MD simulated complexes are shown in green and cyan. For hSERT, the docking pose is represented by gray and the structure from MD is represented by light brown.

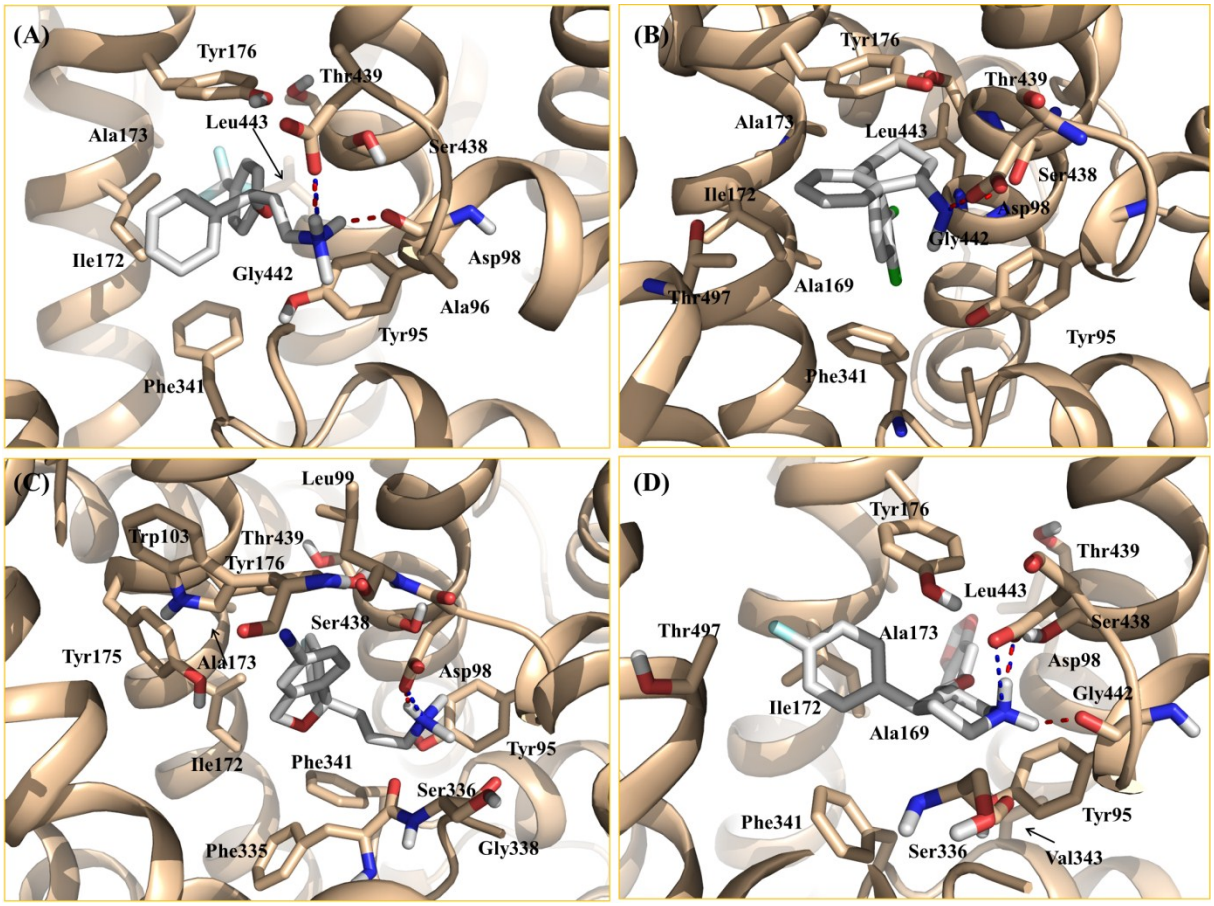

Figure S8. Representative snapshots from MD simulation of 4 studied SSRIs (A) fluoxetine, (B) sertraline, (C) escitalopram and (D) paroxetine with hSERT. The SSRIs and their interacting residues are shown in stick representation, and the protein is shown in cartoon. Salt bridges and hydrogen bonds are depicted as blue and red dotted lines, respectively.

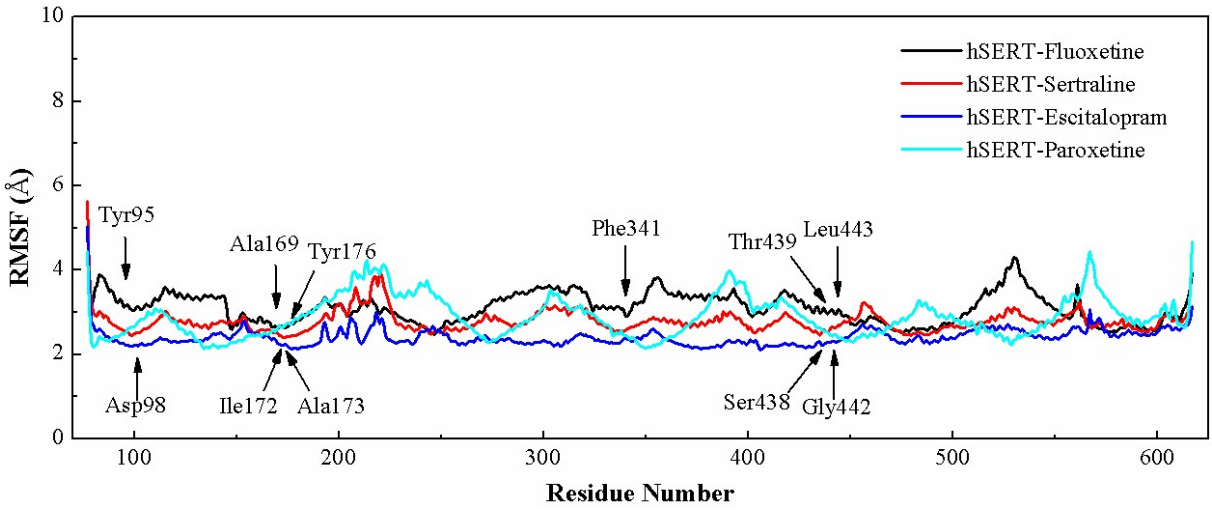

Figure S9. Root mean square fluctuation (RMSF) of the backbone atoms versus residue number for SSRIs bound hSERT.

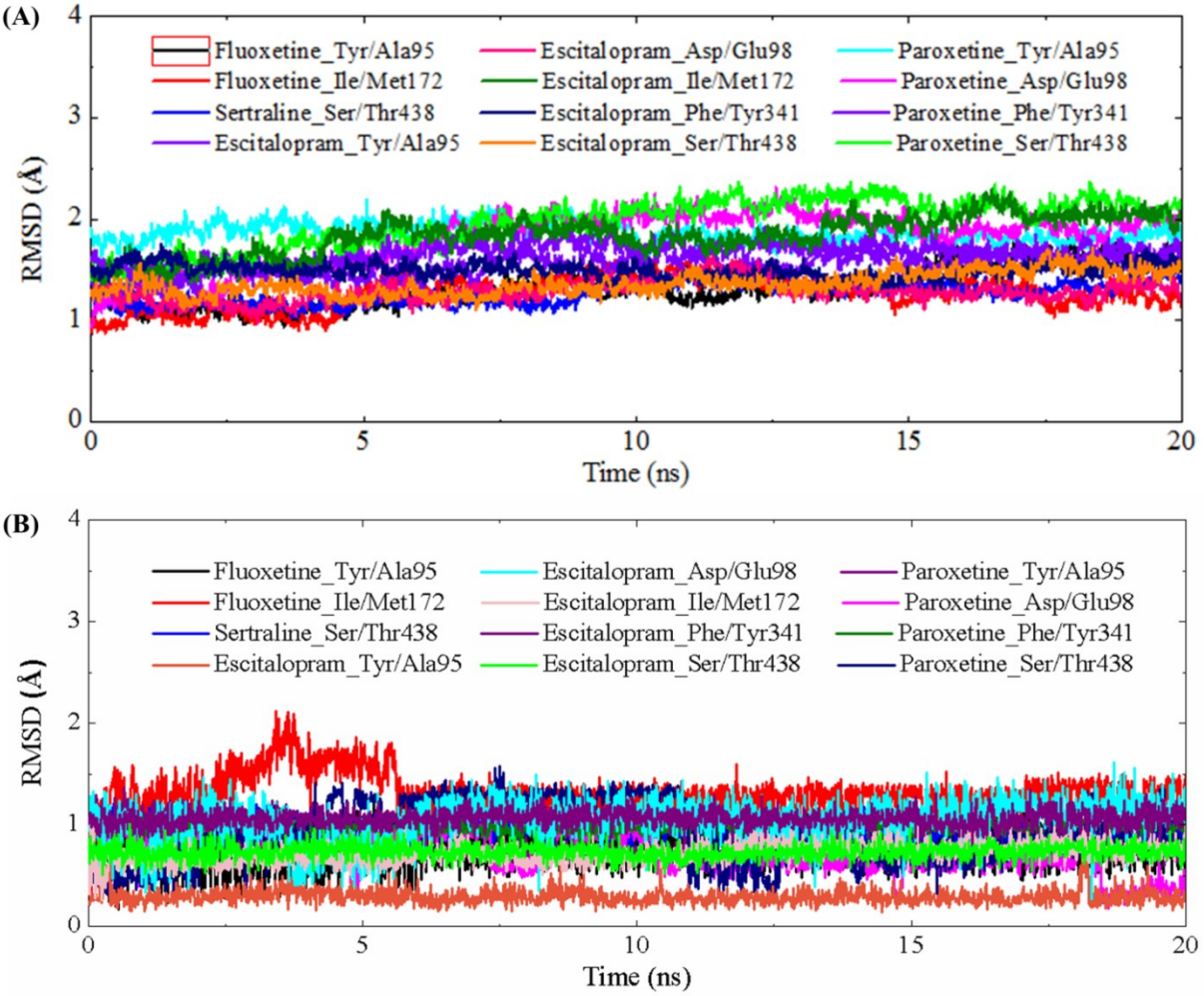

Figure S10. Root mean square deviations of protein backbone atoms (A) and ligand heavy atoms (B) of mutant hSERT as a function of time in MD simulations.

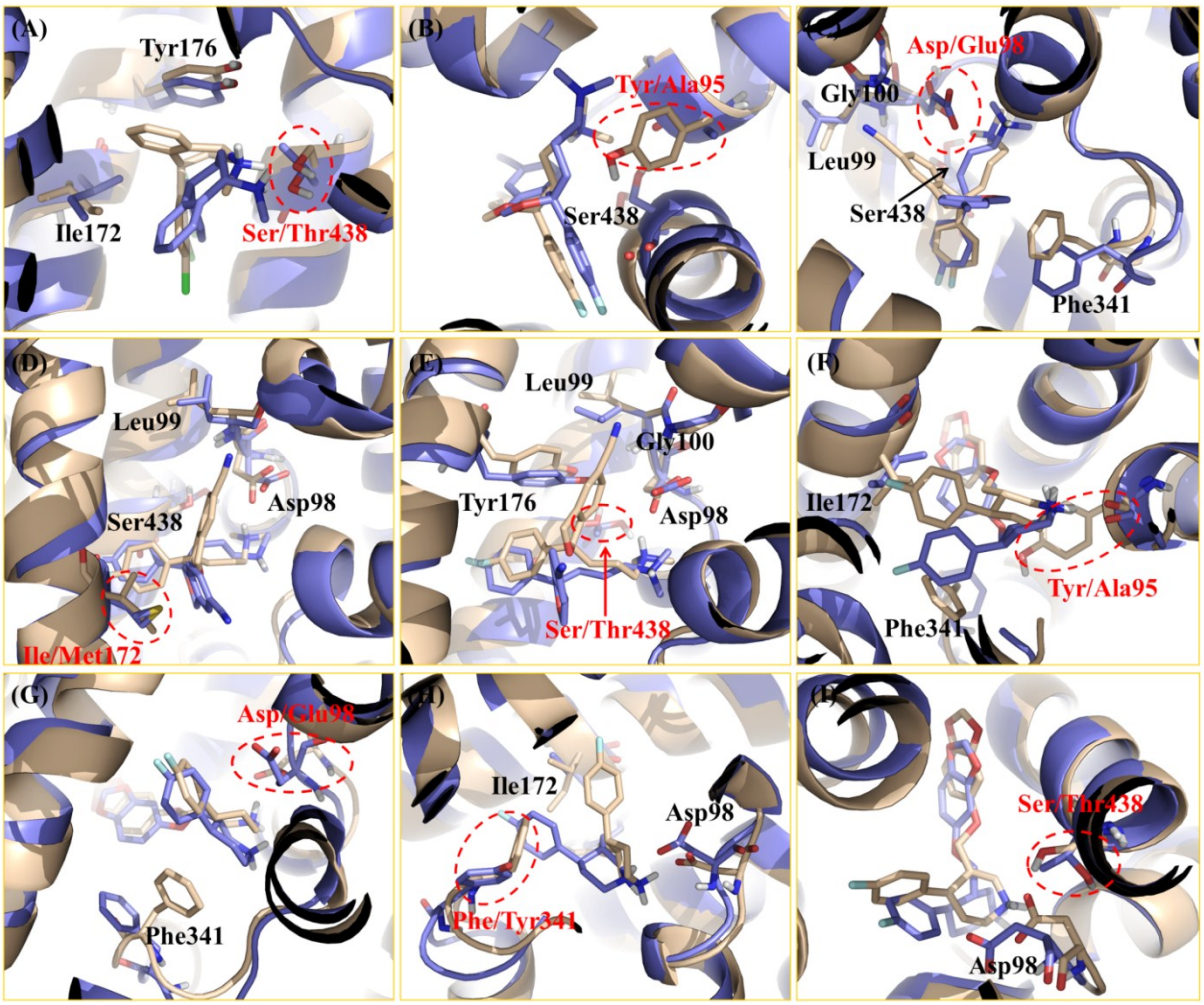

Figure S11. Structural superimposition of (A) sertraline binding to the wild type and Ser/Thr438 mutant hSERT, (B-E) escitalopram binding to the wild type and Tyr/Ala95, Asp/Glu98, Ile/Met172 and Ser/Thr438 mutant hSERTs, (F-I) paroxetine binding to the wild type and Tyr/Ala95, Asp/Glu98, Phe/Tyr341 and Ser/Thr438 mutant hSERT. Residues affected by mutations of hot spot residues and SSRIs are shown as a stick representation in wild type (light brown) and mutant (light blue) models. The mutation residues were highlighted in red dash line circle and font.

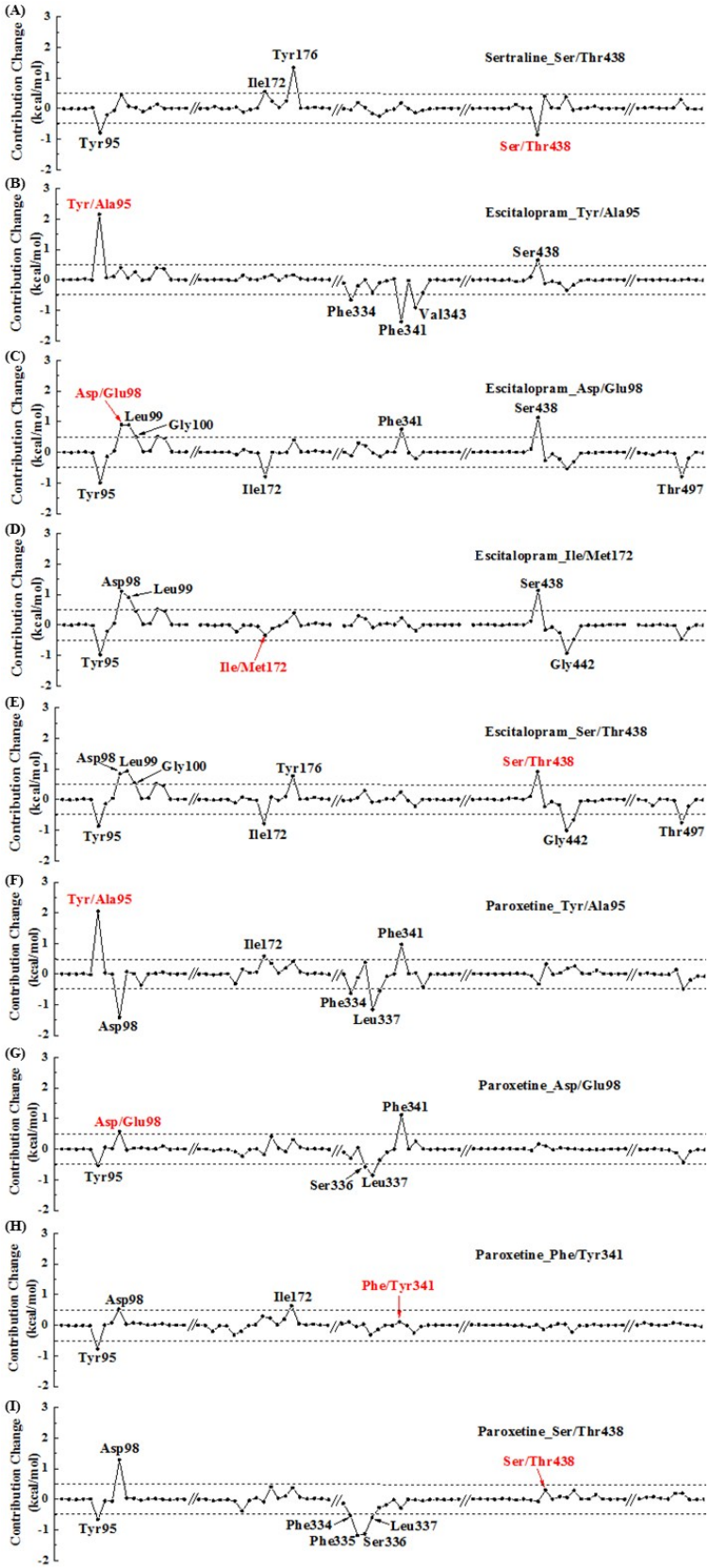

Figure S12. Contribution changes in SSRI's binding by mutation on hot spot residues measured by the per-residue binding free energy corresponding to A-I in ***Figure S9***. The mutation residues were highlighted in red font.

References

1. Glide, version 5.5, Schrödinger, LLC: New York, NY, 2009.
2. LigPrep, version 2.3; Schrödinger, LLC: New York, NY, 2009.
3. G. A. Kaminski, R. A. Friesner, J. Tirado-Rives and W. L. Jorgensen, *The Journal of Physical Chemistry B*, 2001, **105**, 6474-6487.
4. Epik, version 2.0, Schrödinger, LLC: New York, NY, 2009.
5. Maestro, version 9.0, Schrödinger, LLC: New York, NY, 2009.
6. J. Andersen, L. Olsen, K. B. Hansen, O. Taboureau, F. S. Jorgensen, A. M. Jorgensen, B. Bang-Andersen, J. Egebjerg, K. Stromgaard and A. S. Kristensen, *The Journal of biological chemistry*, 2010, **285**, 2051-2063.
7. M. A. Lomize, I. D. Pogozheva, H. Joo, H. I. Mosberg and A. L. Lomize, *Nucleic acids research*, 2012, **40**, D370-376.
8. K. Anwer, J. A. Hovington and B. M. Sanborn, *Biology of reproduction*, 1990, **43**, 851-859.
9. S. Jo, T. Kim, V. G. Iyer and W. Im, *Journal of computational chemistry*, 2008, **29**, 1859-1865.
10. S. Jo, J. B. Lim, J. B. Klauda and W. Im, *Biophysical journal*, 2009, **97**, 50-58.
11. E. L. Wu, X. Cheng, S. Jo, H. Rui, K. C. Song, E. M. Davila-Contreras, Y. Qi, J. Lee, V. Monje-Galvan, R. M. Venable, J. B. Klauda and W. Im, *Journal of computational chemistry*, 2014, **35**, 1997-2004.
12. W. L. Jorgensen, J. Chandrasekhar, J. D. Madura, R. W. Impey and M. L. Klein, *The Journal of chemical physics*, 1983, **79**, 926-935.
13. D.A. Case, J.T. Berryman, R.M. Betz, Q. Cai, D.S. Cerutti, T.E. Cheatham, III, T.A. Darden, R.E.Duke, H. Gohlke, A.W. Goetz, S. Gusarov, N. Homeyer, P. Janowski, J. Kaus, I. Kolossváry, A. Kovalenko, T.S. Lee, S. LeGrand, T. Luchko, R. Luo, B. Madej, K.M. Merz, F. Paesani, D.R. Roe, A. Roitberg, C. Sagui, R. Salomon-Ferrer, G. Seabra, C.L. Simmerling, W. Smith, J. Swails, R.C. Walker, J. Wang, R.M. Wolf, X. Wu, P.A. Kollman, *AMBER 14*; University of California: San Francisco, 2014..
14. V. Hornak, R. Abel, A. Okur, B. Strockbine, A. Roitberg and C. Simmerling, *Proteins*, 2006, **65**, 712-725.
15. C. J. Dickson, B. D. Madej, A. A. Skjevik, R. M. Betz, K. Teigen, I. R. Gould and R. C. Walker, *Journal of chemical theory and computation*, 2014, **10**, 865-879.
16. I. S. Joung and T. E. Cheatham, 3rd, *The journal of physical chemistry. B*, 2008, **112**, 9020-9041.
17. J. Wang, R. M. Wolf, J. W. Caldwell, P. A. Kollman and D. A. Case, *Journal of computational chemistry*, 2004, **25**, 1157-1174.
18. C. I. Bayly, P. Cieplak, W. Cornell and P. A. Kollman, *The Journal of Physical Chemistry*, 1993, **97**, 10269-10280.
19. J. Wang, W. Wang, P. A. Kollman and D. A. Case, *Journal of molecular graphics & modelling*, 2006, **25**, 247-260.

20. M. J. Frisch, H. B. Schlegel, G. E. Scuseria, M. A. Robb, J. R. Cheeseman, G. Scalmani, V. Barone, B. Mennucci, G. A. Petersson, H. Nakatsuji, M. Caricato, X. Li, H. P. Hratchian, A. F. Izmaylov, J. Bloino, G. Zheng, J. L. Sonnenberg, M. Hada, M. Ehara, K. Toyota, R. Fukuda, J. Hasegawa, M. Ishida, T. Nakajima, Y. Honda, O. Kitao, H. Nakai, T. Vreven, J. A. Montgomery, Jr., J. E. Peralta, F. Ogliaro, M. Bearpark, J. J. Heyd, E. Brothers, K. N. Kudin, V. N. Staroverov, R. Kobayashi, J. Normand, K. Raghavachari, A. Rendell, J. C. Burant, S. S. Iyengar, J. Tomasi, M. Cossi, N. Rega, J. M. Millam, M. Klene, J. E. Knox, J. B. Cross, V. Bakken, C. Adamo, J. Jaramillo, R. Gomperts, R. E. Stratmann, O. Yazyev, A. J. Austin, R. Cammi, C. Pomelli, J. W. Ochterski, R. L. Martin, K. Morokuma, V. G. Zakrzewski, G. A. Voth, P. Salvador, J. J. Dannenberg, S. Dapprich, A. D. Daniels, Ö. Farkas, J. B. Foresman, J. V. Ortiz, J. Cioslowski, and D. J. Fox, *Gaussian 09*; Gaussian, Inc.: Wallingford CT, 2009.
21. T. Darden, D. York and L. Pedersen, *The Journal of chemical physics*, 1993, **98**, 10089-10092.
22. W. Humphrey, A. Dalke and K. Schulten, *Journal of molecular graphics*, 1996, **14**, 33-38, 27-38.
23. L. Larini, R. Mannella and D. Leporini, *J Chem Phys*, 2007, **126**, 104101.
24. D. R. Roe and T. E. Cheatham III, *Journal of chemical theory and computation*, 2013, **9**, 3084-3095.
25. The PyMOL Molecular Graphics System, version 1.3, Schrödinger, LLC.
26. P. A. Kollman, I. Massova, C. Reyes, B. Kuhn, S. Huo, L. Chong, M. Lee, T. Lee, Y. Duan, W. Wang, O. Donini, P. Cieplak, J. Srinivasan, D. A. Case and T. E. Cheatham, 3rd, *Accounts of chemical research*, 2000, **33**, 889-897.
27. I. Massova and P. A. Kollman, *Perspectives in drug discovery and design*, 2000, **18**, 113-135.
28. A. Onufriev, D. Bashford and D. A. Case, *Proteins*, 2004, **55**, 383-394.
29. J. Weiser, P. S. Shenkin and W. C. Still, *Journal of computational chemistry*, 1999, 217-230.
30. L. Sorensen, J. Andersen, M. Thomsen, S. M. Hansen, X. Zhao, A. Sandelin, K. Stromgaard and A. S. Kristensen, *The Journal of biological chemistry*, 2012, **287**, 43694-43707.
31. M. A. Larkin, G. Blackshields, N. P. Brown, R. Chenna, P. A. McGettigan, H. McWilliam, F. Valentin, I. M. Wallace, A. Wilm, R. Lopez, J. D. Thompson, T. J. Gibson and D. G. Higgins, *Bioinformatics*, 2007, **23**, 2947-2948.